Article

Stereochemical Nonrigidity of a Chiral Rhodium Boryl Hydride Complex: A σ-Borane Complex as Transition State for Isomerization

Marius V. Cmpian, Eric Clot, Odile Eisenstein, Ulrike Helmstedt, Naseralla Jasim, Robin N. Perutz, Adrian C. Whitwood, and David Williamson

J. Am. Chem. Soc., **2008**, 130 (13), 4375-4385 • DOI: 10.1021/ja077357o

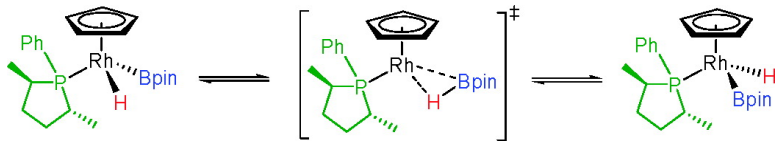

More About This Article

Additional resources and features associated with this article are available within the HTML version:

- Supporting Information
- Access to high resolution figures
- Links to articles and content related to this article
- Copyright permission to reproduce figures and/or text from this article

View the Full Text HTML

J|A|C|S
ARTICLES
Published on Web 03/08/2008

Stereochemical Nonrigidity of a Chiral Rhodium Boryl Hydride Complex: A σ-Borane Complex as Transition State for Isomerization

Marius V. Câmpian,[§] Eric Clot,[#] Odile Eisenstein,*[,#] Ulrike Helmstedt,[#] Naseralla Jasim,[§] Robin N. Perutz,*[,§] Adrian C. Whitwood,[§] and David Williamson[§]

Department of Chemistry, University of York, York YO10 5DD, U.K., and Institut Charles Gerhardt, CNRS, Université Montpellier 2, cc1501, Place E. Bataillon, 34095 Montpellier, France

Received September 23, 2007; E-mail: odile.eisenstein@univ-montp2.fr; rnp1@york.ac.uk

Abstract: Experimental and computational studies are reported on half-sandwich rhodium complexes that undergo B−H bond activation with pinacolborane (HBpin = $HB(OMe_2CMe_2O)$). The photochemical reaction of [Rh(η^5-C_5H_5)(*R,R*-phospholane)(C_2H_4)] **3** (phospholane = PhP(CHMeCH$_2$CH$_2$CHMe)) with HBpin generates the boryl hydride in two distinguishable isomers [(S_{Rh})-Rh(η^5-C_5H_5)(Bpin)(H)(*R,R*-phospholane)] **5a** and [(R_{Rh})-Rh(η^5-C_5H_5)(Bpin)(H)(*R,R*-phospholane)] **5b** that undergo intramolecular exchange. The presence of a chiral phosphine allowed the determination of the interconversion rates (epimerization) by 1D ^{1}H EXSY spectroscopy in C_6D_6 solution yielding $\Delta H^{\ddagger} = 83.4 \pm 1.8$ kJ mol^{-1} for conversion of **5a** to **5b** and 79.1 ± 1.4 kJ mol^{-1} for **5b** to **5a**. Computational analysis yielded gas-phase energy barriers of 96.4 kJ mol^{-1} determined at the density functional theory (DFT, B3PW91) level for a model with PMe_3 and B(OCH_2-CH_2O) ligands; higher level calculations (MPW2PLYP) on an optimized QM/MM(ONIOM) geometry for the full system place the transition state 76.8 kJ mol^{-1} above the average energy of the two isomers. The calculations indicate that the exchange proceeds via a transition state with a σ-B−H-bonded borane. The B−H bond lies in a mirror plane containing rhodium and phosphorus. No intermediate with an η^2-B−H ligand is detected either by experiment or calculation. Complex **3** has also been converted to the [Rh(η^5-C_5H_5)Br$_2$(*R,R*-phospholane)] (characterized crystallographically) and [Rh(η^5-C_5H_5)(H)$_2$(*R,R*-phospholane)]. The latter exhibits two inequivalent hydride resonances that undergo exchange with $\Delta H^{\ddagger} = 101 \pm 2$ kJ mol^{-1}. DFT calculations indicate that the boryl hydride complex has a lower exchange barrier than the dihydride complex because of steric hindrance between the phospholane and Bpin ligands in the boryl hydride.

Introduction

Complexes in which a σ-bond acts as donor to a transition metal are established for dihydrogen, alkanes, silanes, and boranes.[1,2] The evidence for such complexes as ground-state structures is compelling, but they are also increasingly recognized as reaction intermediates or transition states offering routes to chain-walking in alkyl hydride complexes and to isotopic exchange.[2] Some mechanisms, for instance in borylation, can involve multiple σ-complexes that interconvert by dynamic rearrangements.[3] It has recently been postulated that such mechanisms form examples of a new general class of metathesis mechanism termed σ-CAM (σ-complex assisted metathesis).[4] In this paper, we employ a chiral phosphine as an ancillary ligand resulting in products formed as two diastereomers and observe epimerization at the chiral metal center. Our experiments, in combination with density functional theory (DFT) calculations, allow us to infer the existence of an exchange mechanism involving a transition state with a σ-borane ligand; our methodology has potential for other σ-ligands.

[§] University of York.
[#] CNRS, Montpellier.

(1) (a) Kubas, G. J. *Metal Dihydrogen and σ-Bond Complexes*; Kluwer Academic/Plenum Publishers: New York, 2001. (b) Kubas, G. J. *Proc. Nat. Acad. Sci. U.S.A.* **2007**, *104*, 6901. (c) Heinekey, D. M.; Lledós, A.; Lluch, J. M. *Chem. Soc. Rev.* **2004**, *33*, 175. (d) Corey, J. Y.; Braddock-Wilking, J. *Chem. Rev.* **1999**, *99*, 175. (e) Lin, Z. Y. *Chem. Soc. Rev.* **2002**, *31*, 239. (f) Lachaize, S.; Sabo-Etienne, S. *Eur. J. Inorg. Chem.* **2006**, 2115. (g) Crabtree, R. H. *J. Chem. Soc., Dalton Trans.* **2001**, 2437. (h) Sabo-Etienne, S.; Chaudret, B. *Chem. Rev.* **1998**, *98*, 2077. (i) Kubas, G. J. *Catal. Lett.* **2005**, *104*, 79. (j) Maseras, F.; Lledós, A.; Clot, E.; Eisenstein, O. *Chem. Rev.* **2000**, *100*, 601. (k) Lachaize, S.; Caballero, A.; Vendier, L.; Sabo-Etienne, S. *Organometallics* **2007**, *26*, 3713.

(2) (a) Crabtree, R. H. *Angew. Chem., Int. Ed.* **1993**, *32*, 789. (b) Hall, C.; Perutz, R. N. *Chem. Rev.* **1996**, *96*, 3125. (c) Arndtsen, B. A.; Bergman, R. G.; Mobley, T. A.; Peterson, T. H. *Acc. Chem. Res.* **1995**, *28*, 154. (d) Jones, W. D. *Acc. Chem. Res.* **2003**, *36*, 140. (e) Jones, W. D. *Inorg. Chem.* **2005**, *44*, 4475. (f) Lersch, M.; Tilset, M. *Chem. Rev.* **2005**, *105*, 2471. (g) Lawes, D. J.; Geftakis, S.; Ball, G. E. *J. Am. Chem. Soc.* **2005**, *127*, 4134. (h) Ball, G. E.; Brookes, C. M.; Cowan, A. J.; Darwish, T. A.; George, M. W.; Kawanami, H. K.; Portius, P.; Rourke, J. P. *Proc. Nat. Acad. Sci. U.S.A.* **2007**, *104*, 6927. (i) Cowan, A. J.; Portius, P.; Kawanami, H. K.; Jina, O. S.; Grills, D. W.; Sun, X.-Z.; McMaster, J.; George, M. W. *Proc. Nat. Acad. Sci. U.S.A.* **2007**, *104*, 6901. (j) Sun, X. Z.; Grills, D. C.; Nikiforov, S. M.; Poliakoff, M.; George, M. W. *J. Am. Chem. Soc.* **1997**, *119*, 7521. (k) Chen, G. S.; Labinger, J. A.; Bercaw, J. E. *Proc. Nat. Acad. Sci. U.S.A.* **2007**, *104*, 6915. (l) Clot, E.; Eisenstein, O.; Jones, W. D. *Proc. Nat. Acad. Sci. U.S.A.* **2007**, *104*, 6939. (m) Cobar, E. A.; Khaliullin, R. S.; Bergman, R. G.; Head-Gordon, M. *Proc. Nat. Acad. Sci. U.S.A.* **2007**, *104*, 6963.

(3) (a) Hartwig, J. F.; Cook, K. S.; Hapke, M.; Incarvito, C. D.; Fan, Y. B.; Webster, C. E.; Hall, M. B. *J. Am. Chem. Soc.* **2005**, *127*, 2538. (b) Lam, W. H.; Lam, K. C.; Lin, Z. Y.; Shimada, S.; Perutz, R. N.; Marder, T. B. *Dalton Trans.* **2004**, 1556.

(4) Perutz, R. N.; Sabo-Etienne, S. *Angew. Chem., Int. Ed.* **2007**, *46*, 2578.

Enormous progress has been made recently in the catalytic functionalization of simple organic compounds by selective borylation.[5−17] The use of precursors with boron−oxygen bonds (B_2pin_2, HBpin, and their catecholate analogues, pin = pinacolate, $OCMe_2CMe_2O$) that moderate the Lewis acidity of the boron has been central to the progress that has been made. Metal boryl hydride complexes sometimes act as precatalysts in such reactions, for instance in the reactions of [Rh(η^5-C_5Me_5)-(Bpin)$_3$H] and [Ir(η^5-C_5Me_5)(PMe_3)(Bpin)H].[3,11] They serve as intermediates in the catalytic cycles that have been postulated, notably for Rh(η^5-C_5Me_5) and for Ir(Bpin)$_3$ systems (see below).[3,12,15b] They have also been recognized as efficient precursors for catalytic hydroboration and dehydrogenative borylation.[6,18,19] There are several further examples of metal boryl hydride complexes, synthesized both thermally and photochemically.[20−23]

In addition to undergoing oxidative addition, boranes HB-$(OR)_2$ have been shown to coordinate to a metal center while preserving the B−H bond. This type of σ-complex, [M{η^2-HB-$(OR)_2$}],[24] has been characterized crystallographically for HBpin and related compounds; examples include [Ti(η^5-C_5H_5)$_2$(η^2-HBcat)$_2$][25] and various Ru complexes.[26] Such complexes may also play a role in hydroboration[27] and alkane borylation.[28] The σ-CAM mechanism generalizes the pathways involving a series of different σ-ligands as postulated by Hartwig and Hall.[4,28]

The coordination and activation of the B−H bond has been studied computationally.[3,20,29] The relationship between σ-B−H-bonded borane complexes, M{η^2-H−B$(OR)_2$}, and other σ-E-H (E = C, Si, H) ligands has been addressed.[25,26b,29c,30] In particular, the empty p boron orbital has been shown to participate significantly in stabilizing the σ-B−H bond.[29c] The borylation reactions of alkanes and arenes with Mo, W, Ru, Rh, and Ir complexes have been examined,[3a,28,29b,31] and it has been shown that both boryl hydride complexes and σ-B−H complexes are likely to be intermediates in these reactions.

We recently demonstrated that the complexes [Rh(η^5-C_5H_5)-(PR_3)(C_2H_4)] (R = Ph, Me) undergo oxidative addition reactions with HBpin and B_2pin_2 and compared their reactivity toward these boranes to the reactivity with silanes $HSiR_3$.[32] Ampt, Duckett and Perutz have also reported that [Rh(η^5-C_5H_5)(C_2H_4-CO_2tBu)$_2$] undergoes photoreaction with silanes to produce isomeric hydride complexes [Rh(η^5-C_5H_5)(SiR_3)(H)(C_2H_4-CO_2tBu)] that interconvert slowly on the NMR time scale. The results for the trialkylsilanes could be explained by a transition state with an Rh(η^2-H−SiR_3) structure without the need to postulate a corresponding intermediate. However, the differential rate of broadening of the resonances for the two hydride complexes in the cases of trimethoxysilane and chlorodimethylsilane led us to interpret the corresponding isomerization in terms of a Rh(η^2-H−SiR_3) reaction intermediate that epimerized the rhodium center.[33]

The epimerization of half-sandwich complexes M(η^5-C_5H_5)-(X)(Y)(Z) (X ≠ Y ≠ Z) at the metal has been studied, notably by Brunner, Davies, and Gladysz.[34−36] Kinetic and mechanistic

(5) (a) Waltz, K. M.; Hartwig, J. F. *Science* **1997**, *277*, 211. (b) Chen, H.; Schlecht, S.; Semple, T. C.; Hartwig, J. F. *Science* **2000**, *287*, 1995. (c) Chen, H.; Hartwig, J. F. *Angew. Chem., Int. Ed.* **1999**, *38*, 3391.
(6) Murata, M.; Kawakita, K.; Asana, T.; Watanabe, S.; Masuda, Y. *Bull. Chem. Soc. Jpn.* **2002**, *75*, 825.
(7) Cho, J.-Y.; Tse, M. K.; Holmes, D.; Maleczka, R. E.; Smith, M. R., III. *Science* **2002**, *295*, 305.
(8) Shimada, S.; Batsanov, A. S.; Howard, J. A. K.; Marder, T. B. *Angew. Chem., Int. Ed.* **2001**, *40*, 2168.
(9) Ishiyama, T.; Miyaura, N. *J. Organomet. Chem*. **2003**, *680*, 3.
(10) (a) Ishiyama, T.; Takagi, J.; Ishida, K.; Miyaura, N.; Anastasi, N. R.; Hartwig, J. F. *J. Am. Chem. Soc.* **2002**, *124*, 390. (b) Ishiyama, T.; Ishida, K.; Takagi, J.; Miyaura, N. *Chem. Lett.* **2001**, 1082. (c) Takagi, J.; Sato, K.; Hartwig, J. F.; Ishiyama, T.; Miyaura, N. *Tetrahedron Lett.* **2002**, *43*, 5649. (d) Ishiyama, T.; Nobuta, Y.; Hartwig, J. F.; Miyaura, N. *Chem. Commun.* **2003**, 2924. (e) Datta, A.; Köllhofer, A.; Plenio, H. *Chem. Commun.* **2004**, 1508.
(11) (a) Iverson, C. N.; Smith, M. R., III. *J. Am. Chem. Soc.* **1999**, *121*, 7696. (b) Tse, M. K.; Cho, J. Y.; Smith, M. R., III. *Org. Lett.* **2001**, *18*, 2831. (c) Cho, J. Y.; Iverson, C. N.; Smith, M. R., III. *J. Am. Chem. Soc.* **2000**, *122*, 12868. (d) Chotana, G. A.; Rak, M. A.; Smith, M. R., III. *J. Am. Chem. Soc.* **2005**, *127*, 10539.
(12) Lawrence, J. D.; Takahashi, M.; Bae, C.; Hartwig, J. F. *J. Am. Chem. Soc.* **2004**, *126*, 15334.
(13) Dick, A. R.; Sanford, M. S. *Tetrahedron* **2006**, *62*, 2439.
(14) Kurotobi, K.; Miyauchi, M.; Takakura, K.; Murafuji, T.; Sugihara, Y. *Eur. J. Org. Chem.* **2003**, 3663.
(15) (a) Ishiyama, T.; Takagi, J.; Hartwig, J. F.; Miyaura, N. *Angew. Chem., Int. Ed*. **2002**, *41*, 3056. (b) Boller, T. M.; Murphy, J. M.; Hapke, M.; Ishiyama, T.; Miyaura, N.; Hartwig, J. F. *J. Am. Chem. Soc.* **2005**, *127*, 14263.
(16) (a) Coventry, D. N.; Batsanov, A. S.; Goeta, A. E.; Howard, J. A. K.; Marder, T. B.; Perutz, R. N. *Chem. Commun.* **2005**, 2172. (b) Mkhalid, I. A. I.; Coventry, B. N.; Albesa-Jove, D.; Batsanov, A. N.; Howard, J. A. K.; Perutz, R. N.; Marder, T. B. *Angew. Chem., Int. Ed.* **2006**, *45*, 489. (c) Ishiyama, T.; Takagi, J.; Yonekawa, Y.; Hartwig, J. F.; Miyaura, N. *Adv. Synth. Catal*. **2003**, *345*, 1003.
(17) Murphy, J. M.; Lawrence, J. D.; Kawamura, K.; Incarvito, C.; Hartwig, J. F. *J. Am. Chem. Soc*. **2006**, *128*, 13684.
(18) (a) Fernandez, E.; Maeda, K.; Hooper, M. W.; Brown, J. M. *Chem. Eur. J*. **2000**, *6*, 1840. (b) Männing, D.; Nöth, H. *Angew. Chem., Int. Ed.* **1985**, *24*, 878. For reviews see: (c) Burgess, K.; Ohlmeyer, M. J. *Chem. Rev*. **1991**, *91*, 1179. (d) Burgess, K.; van der Donk, W. A. In *Encyclopedia of Inorganic Chemistry*; King, R. B., Ed.; Wiley: Chichester, U.K., 1994; Vol. 3, p 1420. (e) Fu, G. C.; Evans, D. A.; Muci, A. R. In *Advances in Catalytic Processes*; Doyle, M. P., Ed.; JAI: Greenwich, CT, 1995; p 95. (f) Beletskaya, I.; Pelter, A. *Tetrahedron* **1997**, *53*, 4957. (g) Crudden, C. M.; Edwards, D. *Eur. J. Org. Chem.* **2003**, 4695.
(19) For metal catalyzed dehydrogenative borylation of alkenes see: Coapes, R. B.; Souza, F. E. S.; Thomas, R. L.; Hall, J. J.; Marder, T. B. *Chem. Commun.* **2003**, 614 and references therein.
(20) (a) Lam, W. H.; Shimada, S.; Batsanov, A. S.; Lin, Z. Y.; Marder, T. B.; Cowan, J. A.; Howard, J. A. K.; Mason, S. A.; McIntyre, G. J. *Organometallics* **2003**, *22*, 4557. (b) Baker, R. T.; Ovenall, D. W.; Calabrese, J. C.; Westcott, S. A.; Taylor, N. J.; Williams, I. D.; Marder, T. B. *J. Am. Chem. Soc.* **1990**, *112*, 9399. (c) Westcott, S. A; Taylor, N. J.; Marder, T. B.; Baker, R. T.; Jones, N. J.; Calabrese, J. C. *J. Chem. Soc., Chem. Commun.* **1991**, 304. (d) Burgess, K.; van der Donk, W. A.; Westcott, S. A.; Marder, T. B.; Baker, R. T.; Calabrese, J. C. *J. Am. Chem. Soc.* **1992**, *114*, 9350.
(21) Kawamura, K.; Hartwig, J. F. *J. Am. Chem. Soc.* **2001**, *123*, 8422.
(22) Hartwig, J. F.; He, X. M. *Angew. Chem., Int. Ed*. **1996**, *35*, 315. Hartwig, J. F.; He, X. M. *Organometallics* **1996**, *15*, 5350.
(23) Callaghan, P. L.; Fernandez-Pacheco, R.; Jasim, N.; Lachaize, S.; Marder, T. B.; Perutz, R. N.; Rivalta, E.; Sabo-Etienne, S. *Chem. Commun*. **2004**, 242.
(24) (a) Schlecht, S.; Hartwig, J. F. *J. Am. Chem. Soc.* **2000**, *122*, 9435. (b) Muhoro, C. N.; Hartwig, J. F. *Angew. Chem., Int. Ed.* **1997**, *36*, 1510. (c) Muhoro, C. N.; He, X. M.; Hartwig, J. F. *J. Am. Chem. Soc.* **1999**, *121*, 5033. (d) Crestani, M. G.; Munoz-Hernandez, M.; Arevalo, A.; Acosta-Ramirez, A.; Garcia, J. J. *J. Am. Chem. Soc.* **2005**, *127*, 18066.
(25) Hartwig, J. F.; Muhoro, C. N.; He, X. M.; Eisenstein, O.; Bosque, R.; Maseras, F. *J. Am. Chem. Soc.* **1996**, *118*, 10936.
(26) (a) Montiel-Palma, V.; Lumbierres, M.; Donnadieu, B.; Sabo-Etienne, S.; Chaudret, B. *J. Am. Chem. Soc.* **2002**, *124*, 5624. (b) Lachaize, S.; Essalah, K.; Montiel-Palma, V.; Vendier, L.; Chaudret, B.; Barthelat, J.-C.; Sabo-Etienne, S. *Organometallics* **2005**, *24*, 2935.
(27) Hartwig, J. F.; Muhoro, C. N. *Organometallics* **2000**, *19*, 30.
(28) Webster, C. E.; Fan, Y.; Hall, M. B.; Kunz, D.; Hartwig, J. F. *J. Am. Chem. Soc.* **2003**, *125*, 858.
(29) (a) Wan, X. H.; Wang, X. J.; Luo, Y.; Takami, S.; Kubo, M.; Miyamoto, A. *Organometallics* **2002**, *21*, 3703. (b) Tamura, H.; Yamazaki, H.; Sato, H.; Sakaki, S. *J. Am. Chem. Soc.* **2003**, *125*, 16114. (c) Lam, W. H.; Lin, Z. Y. *Organometallics* **2000**, *19*, 2625.
(30) (a) Liu, D.; Lam, K. C.; Lin, Z. Y. *Organometallics* **2003**, *22*, 2827. (b) Pandey, K. K. *J. Organomet. Chem.* **2007**, *692*, 1997. (c) Pandey, K. K. *J. Mol. Struct. (Theochem)* **2007**, *807*, 61.
(31) Lam, W. H.; Lin, Z. Y. *Organometallics* **2003**, *22*, 473.
(32) Câmpian, M. V.; Harris, J. L.; Jasim, N.; Perutz, R. N.; Marder, T. B.; Whitwood, A. C. *Organometallics* **2006**, *25*, 5093.
(33) Ampt, K. A. M.; Duckett, S. B.; Perutz, R. N. *Dalton Trans.* **2004**, 3331.
(34) (a) Brunner, H. *Angew. Chem., Int. Ed.* **1999**, *38*, 1194. (b) Brunner, H.; Zwack, T. *Organometallics* **2000**, *19*, 2423. (c) Brunner, H.; Köllnberger, A.; Mehmood, A.; Tsuno, T.; Zabel, M. *Organometallics* **2004**, *23*, 4006.
(35) Davies, S. G.; Jones, S.; Metzler, M. R.; Yanada, K.; Yanada, R. *J. Chem. Soc., Perkin Trans. 2* **1998**, 1147.
(36) (a) Dewey, M. A.; Stark, G. A.; Gladysz, J. A. *Organometallics* **1996**, *15*, 4798. (b) Saura-Llamas, I.; Gladysz, J. A. *J. Am. Chem. Soc.* **1992**, *114*, 2136.

information can been obtained by NMR spectroscopy if one or more of the ligands is chiral. In one of the few epimerization studies for a hydride complex, Mobley and Bergman showed that a tethered planar chiral cyclopentadienyl iridium cyclohexyl hydride underwent isomerization at 150 °C.[37] Epimerization of [Ir(η^5-C_5Me_5)(H)(dimethylcyclopropyl)(PMe_3)] occurs at a similar temperature, while the rhodium analogue epimerizes at −30 °C.[38,39]

The presence of a suitable phosphine ligand in [Rh(η^5-C_5H_5)(H)(Bpin)(PR_2R')] would allow us to investigate whether rhodium boryl hydride complexes undergo a similar isomerization to their silyl hydride analogues and to determine the barriers between boryl hydride and η^2-borane complexes. Any such epimerization would have important implications for the development of catalysts for the enantioselective borylation of hydrocarbons. For this purpose, we turned to the chiral phospholane, {PhP(2*R*,5*R*-$Me_2C_4H_6$)}, (abbreviated here as *R,R*-phospholane).[40−42] Parkin et al. determined several structures of complexes bearing *R,R*-phospholane and deduced that its electron donating ability lies between those of PPh_3 and PPh_2Me.[43]

In this study, we set out to test the stereochemical rigidity of the rhodium boryl hydride unit. We report the synthesis of the complex [Rh(η^5-C_5H_5)(*R,R*-phospholane)(C_2H_4)], its photochemical reaction in the presence of HBpin, as well as the formation of the dibromide and dihydride complex. We show that [Rh(η^5-C_5H_5)(*R,R*-phospholane)(Bpin)(H)] is formed in two isomeric forms on irradiation of [Rh(η^5-C_5H_5)(*R,R*-phospholane)(C_2H_4)] that interconvert on the NMR time scale. The dihydride complex serves as a reference point for our experimental and computational studies of the boryl hydride complex. Its fluxionality is reminiscent of that of other transition-metal dihydride complexes.[1] We examine the mechanism of the epimerization of the boryl hydride by NMR spectroscopy and by DFT calculations. We show that this intramolecular mechanism, derived by a combination of theory and experiment, illustrates general principles concerning the structure of transition states containing σ-ligands.

Results

A. Synthesis and Spectroscopy. The rhodium phosphine boryl hydride unit [Rh(η^5-C_5H_5)(Bpin)(H)(PR_3)] is chiral at rhodium. While this chirality will not be revealed in an NMR spectrum of a PMe_3 complex, we reasoned that the methyl groups in the PMe_2Ph analogue should be prochiral and yield distinct resonances in the ^1H or ^{13}C NMR spectrum. Synthesis of [Rh(η^5-C_5H_5)(PMe_2Ph)(C_2H_4)] **1** proceeded as expected and photochemical reaction with HBpin at 268 K converted it to [Rh(η^5-C_5H_5)(H)(Bpin)(PMe_2Ph)] **2**. However, the two methyl resonances of **2** were so close together as to preclude quantitative measurement of dynamic behavior. We therefore turned to a chiral phosphine that was capable of generating distinct hydride resonances in the Rh(III) product.

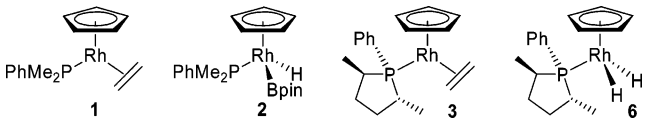

The complex [Rh(η^5-C_5H_5)(*R,R*-phospholane)(C_2H_4)] **3** was synthesized by standard methods from [{Rh(C_2H_4)$_2$}(μ-Cl)]$_2$, (*R,R*-phospholane) and Li(η^5-C_5H_5). It was characterized by multinuclear and 2D NMR spectroscopy. As expected, **3** shows a rhodium-coupled doublet in the $^{31}P\{^1H\}$ NMR spectrum (δ 75.2, d, J_{RhP} = 203 Hz). Its ^1H NMR spectrum was recorded at 700 MHz, and the spectrum was assigned with the aid of COSY and NOESY methods (see Figure S1−S3, Supporting Information). With the aim of obtaining a crystal structure of a derivative, we irradiated **3** at room temperature in the presence of 1,2-dibromoethane (Hg arc, λ > 290 nm) yielding the air stable complex [Rh(η^5-C_5H_5)Br_2(*R,R*-phospholane)] **4** as a single product. When compared with the $^{31}P\{^1H\}$ NMR spectrum of **3**, the spectrum of **4** shows a doublet shifted to high field at δ 49.5 with a reduced value of J_{RhP} (133 Hz), characteristic for a half-sandwich rhodium(III) phosphine dihalide complex.[44] The Supporting Information includes a table (Table S1) with an overview of the principal NMR data.

Slow evaporation of an ether solution yielded red crystals, which were investigated by X-ray crystallography. The crystal structure (Figure 1) confirmed the identity of the product and allowed us to determine its absolute configuration. The puckering of the five-membered ring is indicated by torsion angles P(1)−C(7)−C(8)−C(9) of −30.5(3)° and C(8)−C(9)−C(10)−P(1) of −43.0(3)°. The steric interaction of the phospholane ligand allows orientation of the methyl groups in opposite directions to one another, while the phenyl ring tilts toward the C_5H_5 ring.

Selected bond lengths (Å) and angles (deg) are as follows: Rh(1)−P(1) = 2.2874(9); Br(1)−Rh(1) = 2.5061(7); Br(2)−Rh(1) = 2.5152(8); C(7)−P(1) = 1.857(3); C(10)−P(1) = 1.847(3); C(12)−P(1) = 1.814(3); Rh(1)−C(C_5H_5) = 2.147(3)−2.242(3); Rh(1)−C*g*[C(1)−C(5)] = 1.8227(14); P(1)−Rh(1)−Br(1) = 90.34(3); P(1)−Rh(1)−Br(2) = 89.02(2); Br(1)−Rh(1)−Br(2) = 91.92(1); C(10)−P(1)−Rh(1) = 118.21(9); C(7)−P(1)−Rh(1) = 116.97(9); C(12)−P(1)−Rh(1) = 108.37(9).

An NMR tube was charged with **3** and HBpin (acting as reagent and solvent) and irradiated at room temperature; the reaction was followed by $^{31}P\{^1H\}$ NMR spectroscopy. After irradiation for 3 h, the starting material was converted quantitatively to two products with chemical shifts close to δ 85 and coupling constants of ca. 180 Hz. In contrast to our experience with the PPh_3 analogue where low-temperature irradiation was needed to prevent PPh_3 dissociation, there was no sign of dissociation of the phospholane. All volatiles were removed under vacuum giving a brown oil. On redissolving in C_6D_6, the ^{31}P NMR spectrum was unchanged. ^1H NMR analysis showed that the reaction yields two isomers which differ in the configuration at rhodium [(S_{Rh})-Rh(η^5-C_5H_5)(Bpin)(H)(*R,R*-phospholane)] **5a** and [(R_{Rh})-Rh(η^5-C_5H_5)(Bpin)(H)(*R,R*-phospholane)] **5b** in proportions 2:1, respectively, and minor boron-containing impurities. The reaction is depicted in Scheme 1.

(37) Mobley, T. A.; Bergman, R. G. *J. Am. Chem. Soc.* **1998**, *120*, 3253.
(38) Mobley, T. A.; Schade, S.; Bergman, R. G. *Organometallics* **1998**, *17*, 3574.
(39) Periana, R. A.; Bergman, R. G. *J. Am. Chem. Soc.* **1986**, *108*, 7332.
(40) Burk, M. J. *Acc. Chem. Res.* **2000**, *33*, 363.
(41) Burk, M. J.; Feaster, J. E.; Nugent, W. A.; Harlow, R. L. *J. Am. Chem. Soc.* **1993**, *115*, 10125.
(42) (a) Estevan, F.; Lahuerta, P.; Lloret, J.; Perez-Prieto, J.; Werner, H. *Organometallics* **2004**, *23*, 1369. (b) Estevan, F.; Krueger, P.; Lahuerta, P.; Moreno, E.; Perez-Prieto, J.; Sanau, M.; Werner, H. *Eur. J. Inorg. Chem.* **2001**, 105.
(43) Shin, J. H.; Bridgewater, B. M.; Churchill, D. G.; Parkin, G. *Inorg. Chem.* **2001**, *40*, 5626.
(44) Chin, R. M.; Dong, L.; Duckett, S. B.; Partridge, M. G.; Jones, W. D.; Perutz, R. N. *J. Am. Chem. Soc.* **1993**, *115*, 7685.

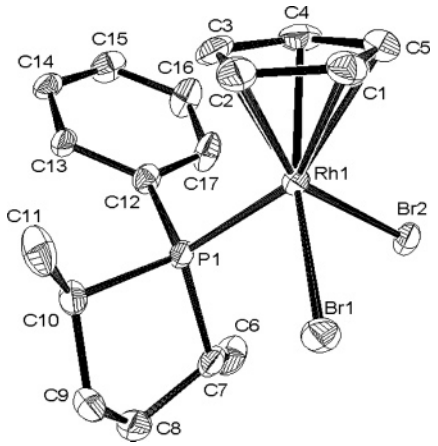

Figure 1. Molecular structure of **4** (50% thermal ellipsoids), all hydrogen atoms omitted.

Scheme 1

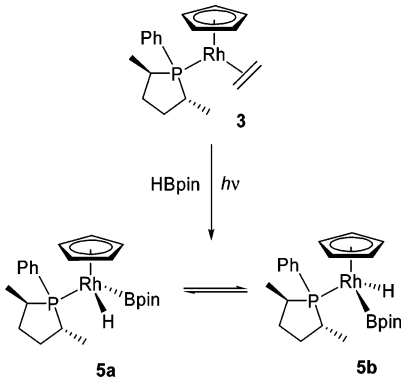

Note that the configurations (*S*/*R*) of the rhodium center have been chosen on the basis of the results of the QM/MM calculations (vide infra).

The hydride region of the ^{1}H NMR spectrum shows two discrete resonances for the isomers at δ −13.6 (**5a**) and −14.3 (**5b**), respectively, each as doublets of doublets with coupling constants J_{HP} ca. 30 Hz and J_{HRh} ca. 35 Hz. The corresponding proton resonances for the five-membered rings are present for both isomers but they overlap, apart from the methyls, which are well resolved as doublets of doublets, and are assigned on the basis of the intensity of the peaks. The methyl resonances belonging to the Bpin ligand and the protons from the C_5H_5 ring appear as singlets (Figure S4).

The ^{31}P{^{1}H} NMR spectrum shows the corresponding two doublets for the isomers with coupling constants characteristic of Rh(III) species[44] (δ 82.6, J_{RhP} 174 Hz; δ 84.7, d, J_{RhP} 179 Hz for **5a** and **5b**, respectively, Figure S5). The ^{11}B NMR spectrum shows a broad resonance at δ 41.7 indicating the formation of the B−H bond activation products.[45]

The equilibrium constants for conversion of **5a** to **5b** were measured by ^{1}H NMR spectroscopy in C_6D_6 as a function of temperature (Table S2). They range from 0.47 at 289 K to 0.55 at 314 K. A Van't Hoff plot yielded $\Delta H^o = 4.3 \pm 0.4$ kJ mol^{-1} and $\Delta S^o = 8.6 \pm 1.4$ J K^{-1} mol^{-1} (Figure 2). The relatively large error bars arise because of the small variation in K_{eq}. We also determined the values in d_8-THF as $\Delta H^o = 7.5 \pm 1.1$ kJ mol^{-1}, $\Delta S^o = 18.0 \pm 3.7$ J K^{-1} mol^{-1}.

(45) Irvine, G. J.; Lesley, G.; Marder, T. B.; Norman, N. C.; Rice, C. R.; Robins, E. G.; Roper, W. R.; Whittell, G. R.; Wright, J. *Chem. Rev.* **1998**, *98*, 2685.

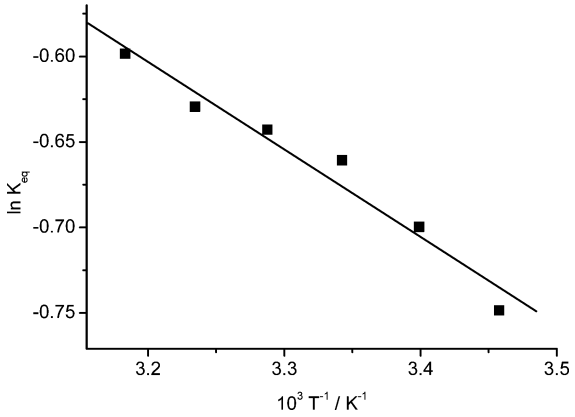

Figure 2. Van't Hoff Plot for equilibrium between **5a** and **5b**.

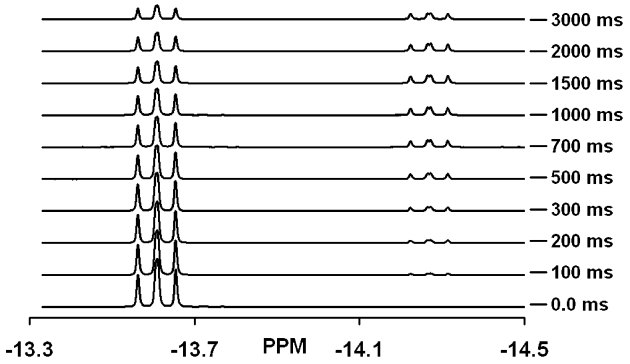

Figure 3. Hydride region of 1D ^{1}H EXSY NMR spectra (700 MHz) of complexes **5a** and **5b** recorded at 314 K in C_6D_6. Mixing times are shown.

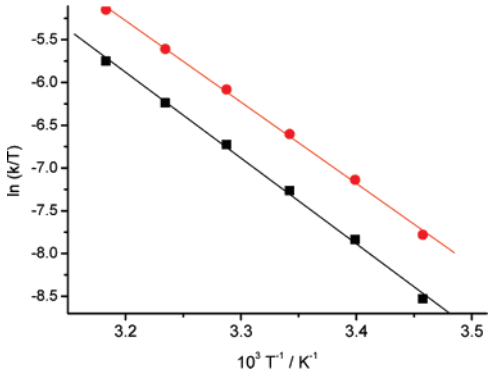

Figure 4. Eyring plot for rate of isomerization of **5b** to **5a** (red) and **5a** to **5b** (black).

Exchange spectroscopy was employed to investigate whether the isomers interconvert on the NMR time scale. 1D ^{1}H EXSY spectra showed that the two hydride ligands exchanged sites slowly at 300 K. A series of EXSY spectra at different temperatures (Figure 3) was recorded to determine rate constants for the interconversion of **5a** and **5b**. The two hydride resonances were excited selectively for mixing times ranging from 0 to 3.0 s. The time evolution of the intensities of the excited peaks and the exchanging peak (each as a ratio of the total intensity) was modeled with a simple exponential function as described in the Experimental Section. The rates were determined between 290 and 315 K; at higher temperatures thermal decomposition prevented satisfactory measurements.

The rate constants are listed in Table S2. An Eyring plot (Figure 4) yielded the activation parameters: $\Delta H^{\ddagger}_{b-a} = 79.1 \pm 1.4$ kJ mol^{-1}, $\Delta S^{\ddagger}_{b-a} = 12 \pm 5$ J K^{-1} mol^{-1}, $\Delta G^{\ddagger}_{b-a,300} =$

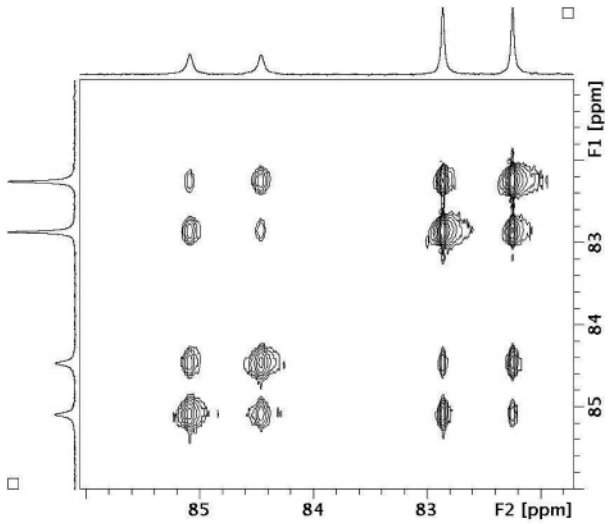

Figure 5. 2D ^{31}P EXSY spectrum (283 MHz) at 300 K showing the exchange between **5a** and **5b** in C_6D_6.

75.5 kJ mol^{-1}; $\Delta H^{\ddagger}_{a-b} = 83.4 \pm 1.8$ kJ mol^{-1}, $\Delta S^{\ddagger}_{a-b} = 20 \pm 6$ J K^{-1} mol^{-1}, $\Delta G^{\ddagger}_{a-b,300} = 77.4$ kJ mol^{-1}.

As a further test of the exchange, 2D ^{31}P{^{1}H} EXSY spectra (283 MHz) were recorded at several temperatures. The spectra clearly show the exchange as off-diagonal peaks and demonstrate the maintenance of ^{31}P-^{103}Rh coupling (Figure 5). Diagonalization of the volume matrices yielded rate constants consistent with those measured by 1D ^{1}H EXSY. The maintenance of coupling strongly suggests that exchange occurs without loss of phosphine. However, we carried out an additional check by adding triphenylphosphine to the sample of **5** in C_6D_6. With [Ph_3P]:**5** = 1:2, we found no evidence of phosphine replacement at room temperature, nor of line broadening of the resonances of **5** or of PPh_3.

We also considered the possibility of solvent participation and repeated the ^{1}H EXSY investigation in THF-d_8 as solvent in place of benzene-d_6. The data showed slightly smaller rate constants and small changes in activation parameters ($\Delta H^{\ddagger}_{b-a} = 73.1 \pm 2.2$ kJ mol^{-1}, $\Delta S^{\ddagger}_{b-a} = -8.3 \pm 7.3$ kJ mol^{-1}; $\Delta H^{\ddagger}_{a-b} = 79.5 \pm 1.1$ kJ mol^{-1}, $\Delta S^{\ddagger}_{a-b} = 6.4 \pm 3.6$ kJ mol^{-1}).

The demonstration of exchange in the boryl hydride complexes **5a** and **5b** led us to synthesize the dihydride analogue, [Rh(η^5-C_5H_5)(H)$_2$(*R,R*-phospholane)] **6** for comparison. This complex was generated by reaction of **4** with $NaBH_4$ in toluene/EtOH followed by purification on an alumina column (adapted from a method of Periana and Bergman).[39] It is characterized by two hydride resonances at δ −13.71 and δ −14.47 that appear as doublets of doublets with similar coupling constants to those for [Rh(η^5-C_5H_5)(H)$_2$(PPh_3)].[32] The ^{31}P NMR spectrum shows a doublet at δ 84.0 with J_{RhP} 159 Hz. In this system, there is the possibility of exchange between the two inequivalent hydrides. Indeed, EXSY spectroscopy demonstrates that such exchange occurs.

The exchange of the two hydride resonances of **6** was studied by 1D ^{1}H EXSY spectroscopy in C_6D_6 over the range 294−314 K (Figure S6). The resulting activation parameters were as follows: $\Delta H^{\ddagger} = 101 \pm 2$ kJ mol^{-1}, $\Delta S^{\ddagger} = 88 \pm 8$ J K^{-1} mol^{-1}, and $\Delta G^{\ddagger} = 74.6$ kJ mol^{-1} (Figure S7). In comparison to the isomer exchange of **5a** and **5b**, the enthalpy of activation and the entropy of activation have both increased leaving the free energy of activation little changed. The high value of $\Delta S^{\ddagger}$ makes it possible that there is some dissociation of phosphine or dihydrogen.

Table 1. Comparison of Calculated and Experimental Geometries (Distances in Å, Angles in deg)

metrics	calculated for **5′**	experimental for [Rh(η^5-C_5H_5)(H)(Bpin)(PPh_3)][32]
Rh−B	2.013	2.0196(15)
Rh−P	2.246	2.2157(4)
Rh−H	1.554	1.50(2)
B···H	2.167	2.09(2)
B−Rh−P	89.7	88.82(4)
H−Rh−B	73.6	71.0(8)
H−Rh−P	85.0	88.5(8)

Theory and Reaction Mechanism. The experimental study demonstrates that **5a** and **5b** interconvert with little dependence on solvent with enthalpies of activation of ca. 80 kJ mol^{-1}. An intramolecular mechanism is indicated by the small entropy of activation, the maintenance of Rh−P, P−H, and Rh−H coupling in the spectra and the lack of effect of added PPh_3. In a first set of calculations, the reaction path for the exchange between the two isomers was investigated with DFT(B3PW91) calculations[46] using PMe_3 instead of the chiral phosphine and ethylene glycolate (O−CH_2−CH_2−O, abbreviated as eg) in place of pinacolate. All species calculated with these simplifications are labeled with slanted prime symbol following the notation.

The achiral phosphine makes the two enantiomers degenerate. The optimized geometry of [Rh(η^5-C_5H_5)(H)(Beg)(PMe_3)] **5′** is in excellent agreement with the geometry of [Rh(η^5-C_5H_5)(H)(Bpin)(PPh_3)], as obtained from X-ray structure analysis.[32] The bond lengths are reproduced to within 0.01 Å for Rh−B and 0.4 Å for Rh−P. The nonbonded B···H distance of 2.167 Å (calcd) and the smaller value for H−Rh−B angle than for H−Rh−P are reproduced excellently (Table 1). The structure of [Rh(η^5-C_5Me_5)(H)(Bpin){P(p-tol)$_3$}] is also similar.[3a]

Three different pathways for the isomerization process have been examined. First, we have looked for oxygen-coordinated intermediates, as previously described by Sakaki et al. and Marder et al.[29b,47] These complexes, resulting from a reductive coupling of boron and hydrogen, could exchange isomers without loss of the borane by rotation about the Rh−O bond. A minimum, 153.5 kJ mol^{-1} above **5′**, [Rh(η^5-C_5H_5)(*O*-HBeg)(PMe_3)] (Figure S8) was located on the potential-energy surface with one oxygen atom coordinated to rhodium.

A second possibility is transfer of H to the C_5H_5 ring with formation of η^4-cyclopentadiene (C_5H_6).[48] Exchange of the isomers would occur by rotation about the Rh-cyclopentadiene axis, as shown in Figure 6. The transition state **TS1′** for the formation of the cyclopentadiene ring has been identified (122.9 kJ mol^{-1} above **5′**). This transition leads to an intermediate η^4-cylopentadiene complex, **Int′**, in which the Rh(I) is in a distorted square planar geometry with P, B, and the two double bonds perpendicular to the coordination plane of the cyclopentadiene (Figure 7). Rotation of the cyclopentadiene requires considerable energy (**TS2′**, 163.8 kJ mol^{-1} above **5′**), presumably because the square planar conformation is transformed into a distorted

(46) (a) Becke, A. D. *J. Chem. Phys.* **1993**, *98*, 5648. (b) Perdew, J. P.; Wang, Y. *Phys. Rev. B* **1992**, *45*, 13244.
(47) Lam, K. C.; Lin, Z. Y.; Marder, T. B. *Organometallics* **2007**, *26*, 3149.
(48) Jones, W. D.; Rosini, G. P.; Maguire, J. A. *Organometallics* **1999**, *18*, 1754.

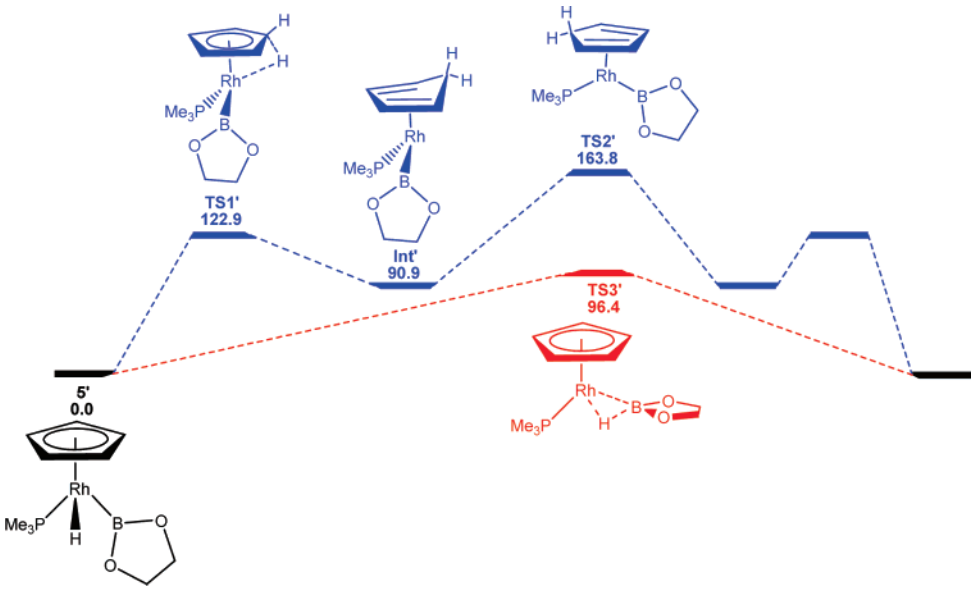

Figure 6. Electronic energy profiles (kJ mol^{-1}) for exchange of boryl hydride isomers of **5′** for the hydrogen transfer to Cp pathway (blue) and the η^2-B−H pathway (red).

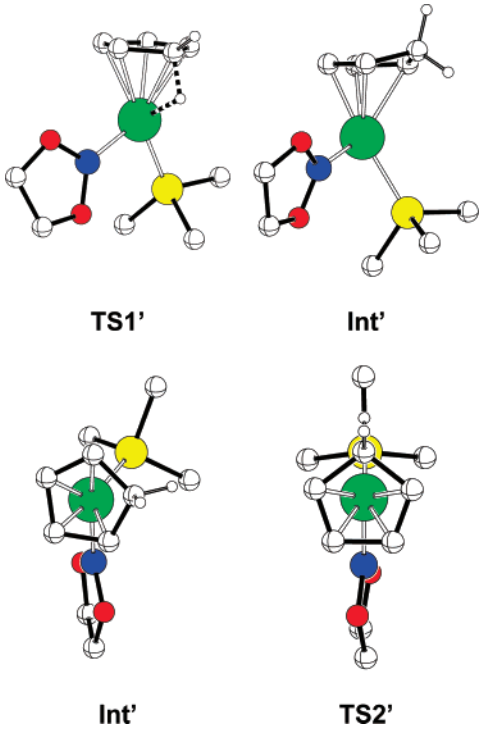

Figure 7. Optimized geometries for the minimum (**Int′**) and transition states (**TS1′** and **TS2′**) for the transport of the H atom via the cyclopentadienyl ring. Above, side views of **TS1′** and **Int′**; below, top views of **Int′** and **TS2′**. All hydrogen atoms have been omitted for clarity with the exception of the migrating H and the geminal H.

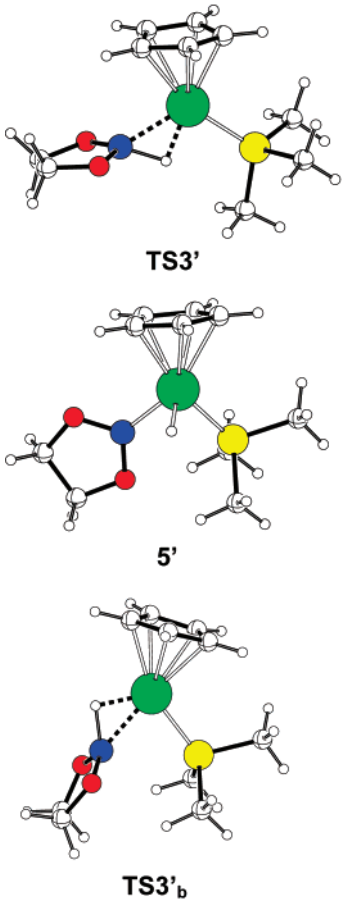

Figure 8. Calculated ground-state geometry of [Rh(η^5-C_5H_5)(H)(Beg)-(PMe_3)] **5′** and geometries of transition states for isomerization. **TS3′** is at lower energy than **TS3′$_b$**.

tetrahedral structure, very unfavorable for tetracoordinated Rh(I).

Third, we have searched for a pathway involving B−H bond formation and located a transition state **TS3′** with B−H coordination 96.4 kJ mol^{-1} above **5′** (Figure 6). The associated $\Delta H^{\ddagger}$ of 94.6 kJ mol^{-1} compares to the average experimental value for the two enantiomers of 81.5 kJ mol^{-1}. In **TS3′** the B−H distance is 1.326 Å, which is significantly shorter than the B···H distance in **5′** (2.167 Å) and longer than in optimized isolated H−Beg (1.188 Å) (Figure 8). The Rh−H distance is 1.646 Å and the Rh−B bond 2.152 Å, compared to 1.554 Å and 2.013 Å in **5′**. The average plane of the glycolate lies parallel to the η^5-C_5H_5 ring. The angle (midpoint O,O)−B−Rh is 162° in **TS3′** compared to 177° in **5′**; a reduction characteristic of a σ-borane complex.[26] The geometry of **TS3′** can be thus described as a σ-B−H complex of H−Beg. It has a local mirror

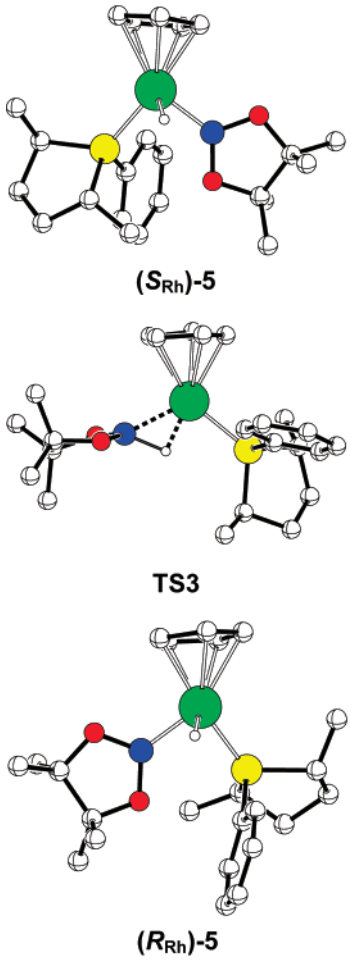

Figure 9. Optimized QM/MM structures of (S_{Rh})-**5** and (R_{Rh})-**5** and the transition state **TS3** for isomerization. All hydrogen atoms bonded to carbons have been omitted for clarity.

plane containing Rh, H, B, and P, showing the appropriate structure to exchange chirality at the metal center. Considering that **TS3′** lies at much lower energy than the transition states for the first two mechanisms (see above), we assign **TS3′** as the transition state for the isomerization and eliminate the O-coordination and the hydrogen-transfer mechanisms.

A second transition state, **TS3′$_b$**, was located 15.5 kJ mol^{-1} above **TS3′**, in which the σ-borane ligand is rotated by 180° about the Rh−borane axis. This rotamer of **TS3′** should behave very similarly to **TS3′** and it has not been considered further.

QM/MM optimizations were carried out for (S_{Rh})-**5**, (R_{Rh})-**5**, and **TS3** with the experimental substituents to account for their steric contributions to the energies. They show that the (S_{Rh}) enantiomer of **5** is more stable than the (R_{Rh}) enantiomer by 14.5 kJ mol^{-1} (Figure 9). The difference in energy is reduced to only 1.8 kJ mol^{-1} in favor of the same isomer when the energies of the structures optimized at the QM/MM level are calculated at the DFT level. The different values arise from different treatment of C−H···π-stacking interactions (2.992−3.337 Å) between the phenyl group on the phospholane and one methyl group on the Bpin ligand, which are underestimated with DFT and overestimated with the MM force field. Thus, the two energy values bracket the experimental quantity of 4.3 ± 0.4 kJ mol^{-1}. The transition state for isomerization, **TS3**, was located at the QM/MM level at 72.1 kJ mol^{-1} above the (S_{Rh})-**5** isomer. Single-point calculations of this transition state at the DFT level give an energy barrier of 62.8 kJ mol^{-1} above the most stable isomer, which may be compared with the experimental value of 83.4 kJ mol^{-1}. Its geometry remains essentially identical to that of **TS3′**. However, because of the chiral phospholane, **TS3** no longer has a mirror plane. Nevertheless, its η^2-B−H unit is almost coplanar with the Rh−P bond as shown by the torsion angle P−Rh−B−H of 5°.

A natural bonding orbital (NBO) analysis shows that **TS3′** can be described as a Rh(I) complex with four lone pairs on Rh, while **5′** is a Rh(III) complex with only three lone pairs on Rh, as expected for d^8 and d^6 complexes, respectively. In **TS3′** the σ(B−H) NBO population is 1.67 e compared to 1.98 e in free HBeg. The σ(B−H) bond donates into a vacant Rh orbital which is significantly antibonding with the Cp ring (σ-Rh hybrid in Figure 10). Consequently, the σ(B−H) natural localized molecular orbital (NLMO) exhibits a significant contribution from Rh (11.5%), while preserving 82% of its parent NBO character.

Only one lone pair on Rh, LP(Rh^{I}) (Figure 10), is involved in back-donation to the borane ligand which accepts electrons both into its vacant p and its σ*(B−H) orbitals. The interaction energies (evaluated by second-order perturbation theory) of this lone pair with σ*(B−H) and the empty p orbital are 59.0 and 56.1 kJ mol^{-1}, respectively. The similar values arise because the larger energy gap between the Rh lone pair and σ*(B−H) is compensated by a larger overlap term for these two orbitals than for interaction between the Rh lone pair and the vacant B(p) orbital.

Backbonding to the boryl group is less efficient in **5′** than in **TS3′**, as shown by the interaction energy of 34.7 kJ mol^{-1}. The energy gap between (LP)Rh and B(p) is similar to that in **TS3′**, but the interaction term is reduced. Consequently, the NLMO for LP(Rh^{III}) shows less delocalization between Rh and B for **5′** (1.5% B) than that for LP(Rh^{I}) in **TS3′** (5.1%).

The dihydride complex **6** serves as a reference for comparison to the boryl hydride complex **5**, and computational studies were carried out similarly. The structures of **6′** (phosphine = PMe_3) and the transition state for H/H exchange **TS4′** have been optimized at the DFT level (Figure 11). The complex **6′** has an octahedral geometry with a mirror plane containing P, Rh, and the cyclopentadienyl centroid. The angles H−Rh−H and P−Rh−H are 77° and 83°, respectively, and there is no short contact between the two hydrogens (Rh−H = 1.552, H···H = 1.924 Å) or between H and the phosphine. The transition state has an η^2-coordinated dihydrogen ligand (H−H = 0.863, Rh−H (av) = 1.680 Å) occupying the mirror plane of the complex. The energy barrier for the H/H exchange is calculated as 97.2 kJ mol^{-1}.

Introduction of the experimental phospholane at the QM/MM level provides structures for the full dihydride complex **6** and the associated transition state **TS4**. The geometries are barely changed with respect to the model systems **6′** and **TS4′**. **TS4** no longer has a formal mirror plane but the torsion angle P−Rh−H−H is only 2.4°. The energies obtained from single point DFT calculations on the QM/MM geometry give a barrier for H/H exchange of 101.7 kJ mol^{-1}.

Discussion

Epimerization of 5. Our experimental studies show that the boryl hydride **5** is formed in two isomeric forms, **5a** and **5b**,

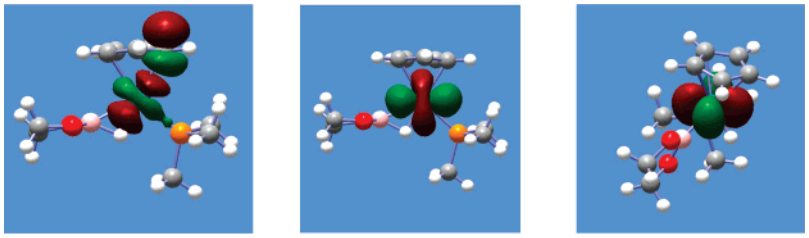

Figure 10. Natural bonding orbitals on Rh: (left) **TS3′**, σ-Rh hybrid accepting from B−H; (center) **TS3′**, LP(Rh^{I}) π-back-donating to the borane; and (right) **5′**, LP(Rh^{III}) π-back-donating to boryl.

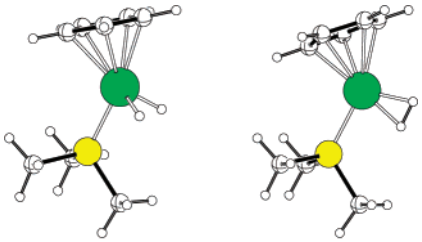

Figure 11. Optimized geometries at the DFT level for [Rh(η^5-C_5H_5)$(H)_2$-(PMe_3)] **6′** and for the transition state **TS4′** for H/H exchange.

with opposite configurations at rhodium, that undergo intramolecular epimerization with $\Delta H^{\ddagger}_{b-a} = 79.1 \pm 1.4$ kJ mol^{-1} and $\Delta H^{\ddagger}_{a-b} = 83.4 \pm 1.8$ kJ mol^{-1}. Epimerization of **5** requires passage through a structure in which the boron and hydrogen atoms are in the approximate mirror plane containing Rh, P, and the center of the cyclopentadienyl ligand. The {Rh(η^5-C_5H_5)(phospholane)} fragment is a d^8 ML_4 fragment with a butterfly geometry that can bond only one ligand in the "mirror" plane. Thus, a reductive coupling of H and Beg has to occur to form a coordinated B−H σ-bond in the transition state. The resulting structure has been characterized as such both with the model and the complete substituents. This structure converts to the d^6 configuration with the pseudooctahedral structure for **5** (or **5′**) through oxidative cleavage.

An intermediate with an η^2-B−H ligand would be expected to have the B−H bond orthogonal to the Rh−P bond and to be asymmetric. No such intermediate could be located as minimum on the potential energy surface and all attempts lead back to the boryl hydride complex. The only minimum lying at relatively low energy has an oxygen atom bonded to the metal. Since this minimum is already at higher energy than the transition state with coordinated B−H bond, we deduce that the isomerization occurs in one step through the transition state with an η^2-B−H bond without passing through any intermediate. The alternative pathway involving H transfer to C_5H_5 also involves a transition state at much higher energy.

Comparison of the Energy Barriers for H/Boryl and H/H Exchange. The experimental value of $\Delta H^{\ddagger} = 101 \pm 2$ kJ mol^{-1} for H/H exchange in **6** is significantly higher than that for B/H exchange in **5** (average $\Delta H^{\ddagger} = 81.5 \pm 2$ kJ mol^{-1}), but the dihydride result is complicated by a high value of $\Delta S^{\ddagger}$, which could indicate partial dissociation of H_2 or phospholane. The computational results for exchange at **5** and **6** depend on the nature of the ligands used in the calculations. When the calculations are carried out with the small ligands, the energy barrier for H/boryl ($\Delta E^{\ddagger} = 96.4$ kJ mol^{-1}) is very close to the barrier for H/H exchange (97.2 kJ mol^{-1}). A difference in barriers is found only when the true ligands are introduced ($\Delta(\Delta E^{\ddagger})_{calcd} = 39.8$ kJ mol^{-1} versus $\Delta(\Delta H^{\ddagger})_{exp} = 20$ kJ mol^{-1}; DFT(B3PW91) calculations on the QM/MM optimized geometries). This result arises because the energy barrier is lowered significantly from 96.4 to 61.9 kJ mol^{-1} (average *R*- and *S*-isomers) in the boryl hydride case by the full ligand set, whereas the energy barrier in the dihydride complex is hardly changed. Considering the known deficiencies of frequently used pure and hybrid functionals (e.g., B3LYP and B3PW91) in reproducing weak interactions,[49] the double hybrid functional MPW2PLYP, recently proposed by Grimme et al.,[50] was used in single point calculations on the QM/MM geometries to estimate the energy barrier. This functional, which adds an MP2 correction to the Kohn−Sham density, gives an average energy barrier (average *R*- and *S*-isomers) for H/H exchange in **6** of 101.7 kJ mol^{-1} and for the H/B exchange in **5** of 76.8 kJ mol^{-1}, in better agreement with the experimental values.

Table 2. Energies of Formation ΔE from Rh(η^5-C_5H_5)L + Borane or H_2 of the Boryl Hydride and Dihydride Complexes and Associated Transition States for Exchange (kJ mol^{-1})

	species	ΔE (DFT) small ligands	ΔE (DFT/QM/MM)[a] full ligands	ΔE (DFT/QM/MM)[a] − ΔE (DFT)
boryl hydride	(S_{Rh})-**5** or **5′**	−210.1	−148.6	61.5
TS for B/H exchange	**TS3** or **TS3′**	−113.9	−85.4	28.5
dihydride	**6** or **6′**	−203.0	−180.4	22.6
TS for H/H exchange	**TS4** or **TS4′**	−105.5	−78.7	26.9

[a] DFT/QM/MM: DFT(B3PW91) calculations on QM/MM optimized geometries.

For a more detailed analysis, we use the separated fragments Rh(η^5-C_5H_5)L and the borane/dihydrogen as the energetic origins (Table 2). Steric factors destabilize the boryl hydride complex strongly as shown by its energy of formation which is about 61.5 kJ mol^{-1} less with the full ligand set ((S_{Rh})-**5**) than with the small ligand set (**5′**). In contrast, the full ligand set influences the transition states, **TS3** and **TS3′**, less since they differ by only 28.5 kJ mol^{-1}. In the case of the dihydride, the full set of ligands has about the same effect on the ground state and the transition state as they are both destabilized by about 25 kJ mol^{-1} with the full ligand set. Therefore, the lower energy barrier for H/boryl relative to H/H exchange arises from larger steric hindrance between the phospholane and the borane in the boryl hydride complex.

Comparison of the Transitions States for H/B and H/H Exchange: NBO Analysis. It is somewhat surprising that the

(49) Sousa, F. S.; Fernandes, P. A.; Ramos, M. J. *J. Phys. Chem. A* **2007**, *111*, 10439.
(50) Schwabe, T.; Grimme, S. *Phys. Chem. Chem. Phys.* **2007**, *9*, 3397.

energy barriers for H/borane and H/H exchange are so similar when the steric effects are not included, since one would expect a special stabilizing effect at the H/boryl transition state due to backbonding into the vacant p-orbital at the boron center in addition to the backbonding into σ^*(B−H). An NBO analysis for the H/boryl and H/H transition states gives an interpretation of this result. Even though the σ-donation from H−H is comparable to that from the B−H bond (451.7 and 450.8 kJ mol^{-1}), the situation for back-donation differs significantly. Comparison of the second-order perturbation energies, shows that the back-donation to σ^*(H−H) is significantly more stabilizing than back-donation to σ^*(B−H) (91.7 and 58.9 kJ mol^{-1} for σ^*(H-H) and σ^*(B−H), respectively). The stronger interaction energy for the H_2 ligand compensates in large part for additional donation into the empty p orbital of the borane and results in similar energy barriers for the two systems, if steric effects are excluded. This result illustrates the well-recognized fact that the spherical nature of the s orbital of the hydrogen atom makes H_2 especially efficient for interacting with a metal center in an η^2-bonding mode.[51] The B−H bond, which uses boron s and p orbitals is more directional and interacts less efficiently with the metal center.

Conclusion

In this work we have shown that a chiral half-sandwich rhodium boryl hydride complex undergoes epimerization at rhodium via a transition state with a σ-borane ligand. The study highlights several more general principles. The use of an asymmetric phosphine reveals the existence of the intramolecular isomerization pathway. The hydride resonances of the two isomers are well separated ($\Delta\delta$ 0.7 ppm) allowing us to employ EXSY techniques to determine rates and activation parameters. The experimental observations, in combination with DFT calculations, enabled us to determine the isomerization pathway and indicate unambiguously that the transition state involves a σ-complex with an η^2-H-Bpin ligand as the key structure. The transition state has a structure in which Rh, P, H, and B occupy the same plane facilitating epimerization. There is no intermediate (minimum) with an η^2-H-Bpin ligand. Our previous experimental study of isomerization of silyl hydrides provided no distinction between an η^2-Si−H intermediate and η^2-Si−H transition state for [Rh(η^5-C_5H_5)(η^2-$C_2H_3CO_2t$Bu)($SiEt_3$)(H)], but it did provide evidence for the existence of an intermediate in the $Si(OMe)_3$ and $SiMe_2Cl$ analogues.[33]

We have also synthesized the corresponding dihydride complex and shown that it undergoes H/H exchange with an appreciably higher value of $\Delta H^{\ddagger}$, but also with a higher $\Delta S^{\ddagger}$ than the values for B/H exchange in **5**. Calculations indicate a pathway for exchange like that for the boryl hydride, but with a transition state containing a rhodium−dihydrogen bond. Exchange of hydrides in polyhydride complexes has been shown to go via an η^2-H_2-bonded transition state.[1k] The analysis of the computational results shows that origin of the lower barrier of boryl hydride lies in steric hindrance in the boryl hydride complex.

We show above that the transition states for epimerization for d^6 [Rh(η^5-C_5H_5)(E)(H)(L*)] species result from reductive coupling of the E−H bond (E = H, B), that is, they are of the type d^8 [Rh(η^5-C_5H_5)(η^2-E-H)(L*)] species where the E−H ligand lies in the plane Rh(η^5-C_5H_5)$_{centroid}$L*.

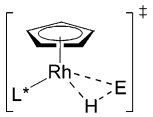

The relatively rapid epimerization at rhodium suggests that catalytic reactions featuring chiral half-sandwich boryl hydride complexes are unlikely to be suitable for asymmetric induction if they depend on maintaining chirality at rhodium. It should be possible to use the same methods to test for the existence of analogous pathways for related species with other nonmetals in place of boron. Since the diastereomers are generated through the use of a relatively simple cyclic phosphine, the methodology is very general and represents only a slight change from standard half-sandwich complexes. It also offers the advantage of access to ^{31}P NMR spectroscopy. Our previous use of η^2-*tert*-butylacrylate as a co-ligand introduced potential hydrogen transfer pathways,[33] while the activation of cyclopropyl derivatives cannot be generalized to B−H and Si−H activation.[39]

Experimental Section

General Procedures. All operations were performed under a nitrogen or argon atmosphere, either on a high-vacuum line (10^{-4} mbar), standard Schlenk (10^{-2} mbar) lines, or in a glovebox. Solvents for general use (THF, benzene, toluene) were of AR grade, dried by distillation over sodium, and stored under Ar in ampules fitted with a Young's PTFE stopcock. Deuterated solvents were dried by stirring over potassium and distilled under high vacuum into small ampules with potassium mirror. *R,R*-Hexanediol was obtained from Fluka, HBpin and LiC_5H_5 from Aldrich, and phenylphosphine and dimethylphenylphosphine from Strem.

Photochemical reactions at room temperature were performed in pyrex NMR tubes fitted with Young's PTFE stopcocks by using a 125 W medium-pressure mercury vapor lamp with a water filter (10 cm). UV−vis irradiations at lower temperatures were performed using a 300 W Oriel 66011 xenon lamp with a thermostatically controlled cooling system based on gaseous nitrogen boil-off.

All standard NMR spectra were recorded on AMX500 spectrometers, unless otherwise stated, in tubes fitted with Young's PTFE stopcocks. All ^{1}H and ^{13}C chemical shifts are reported in ppm (δ) relative to tetramethylsilane and referenced using the chemical shifts of residual protio solvent resonances (benzene, δ 7.16). The ^{31}P{^{1}H} NMR spectra were referenced to external H_3PO_4, ^{11}B NMR spectra to external BF_3·Et_2O.

Mass spectra were recorded on a VG-Autospec spectrometer and are quoted for ^{11}B. Microanalyses were carried out by Elemental Microanalysis Ltd.

EXSY Spectroscopy. All EXSY NMR data were collected on a Bruker Avance II 700 MHz spectrometer, using a broadband inverse geometry probe. For a variable temperature study of the exchange rate, 1D ^{1}H EXSY (*selnogp*)[52] experiments were used. These experiments employ shaped pulses to select the resonances associated with the hydride of the major isomer. The resulting spectrum is effectively a single line of a 2D-EXSY spectrum. The peak at the resonance frequency of the major isomer corresponds to the diagonal peak of the 2D spectrum while the peak at the frequency of the minor isomer corresponds to the cross-peak. To determine the exchange rate at a given temperature, experiments were carried out at 10 mixing times

(51) Saillard, J. Y.; Hoffmann, R. *J. Am. Chem. Soc.* **1984**, *106*, 2006.

(52) (a) Kessler, H.; Oschkinat, H.; Griesinger, C.; Bermel, W. *J. Magn. Reson.* **1986**, *70*, 106. (b) Stonehouse, J.; Adell, P.; Keeler, J.; Shaka, A. J. *J. Am. Chem. Soc.* **1994**, *116*, 6037. (c) Stott, K.; Stonehouse, J.; Keeler, J.; Hwang, T. L.; Shaka, A. J. *J. Am. Chem. Soc.* **1995**, *117*, 4199.

t_{mix} of 0, 100, 200, 300, 500, 700, 1000, 1500, 2000, and 3000 ms. Experiments were carried out at nominal temperatures of 290, 295, 300, 305, 310, and 315 K. The temperature was calibrated using 80% 1,2-ethanediol in d_6-DMSO, following the manufacturer's recommended method.

The peak integrals were determined using the manufacturer's software. The sum of these integrals provides a measure of the total magnetization. Assuming a simple two-site exchange model a ⇌ b, the decay of the diagonal peak integral relative to the total magnetization can be represented by the exponential

$$[B] = [B]_{inf}(1 - \exp(-kt_{mix})) \quad (1)$$

where [B] is the integral of the cross-peak divided by the total magnetization at mixing time t_{mix} and $[B]_{inf}$ is the integral of the cross-peak at infinite mixing time (the equilibrium value). [A] is the integral of the diagonal peak divided by the total magnetization and is equal to 1 − [B]. For the two site exchange model, $k = k_{ab} + k_{ba}$, where k_{ab} and k_{ba} are the forward and reverse rate constants. $[A]_{inf}$, the equilibrium value of the diagonal peak integral relative to the total magnetization is equal to $1 - [B]_{inf}$. The equilibrium constant was determined from the ratio of the integrals of the hydride resonances on a standard ^{1}H NMR spectrum. Equilibrium constants, K_{eq}, derived from the infinite time values of [A] and [B] were consistent with simple integration but less accurate. The values of k_{ab} and k_{ba} were determined from $K_{eq} = k_{ab}/k_{ba}$ and the above equation for k. Finally, the rate constants obtained from the simulation were multiplied by 2 to take account of the possibility of returning from the transition state to the starting isomer.[53] The Eyring analysis was carried out in Microcal Origin 6.1. Standard error bars were taken directly from linear fitting of the plots of ln k/T versus $1/T$.

The 2D ^{31}P−^{31}P EXSY experiments were carried out using the phase sensitive EXSY sequence (*noesygpph*, acquisition time ca. 15 h)[54,55] with proton decoupling centered on the hydride region during the acquisition period. Since exchange was expected to be relatively slow, the mixing time was set at 2 s. By collecting a further 2D EXSY data set with zero mixing time the exchange rates were determined by diagonalization of the volume matrix as described by Perrin and Dwyer.[56]

Syntheses and NMR Experiments. [Rh(η^5-C_5H_5)(PMe_2Ph)(C_2H_4)] 1. The complex was synthesized in a similar manner to the literature procedure, but replacing Tl(η^5-C_5H_5) by Li(η^5-C_5H_5).[57,58] (C_6D_6, 300 K), ^{1}H: δ 7.63−7.10 (m, 10 H, C_6H_5), 5.11 (s, C_5H_5), 2.82 (m, 2H, C_2H_4), 1.48 (m, 2H, C_2H_4), 1.11 (dd, J_{PH} = 8.7, J_{RhH} = 1.1 Hz, 6H, PMe_2Ph). ^{31}P{^{1}H}: δ 21.0 (d, J_{RhP} = 204 Hz).

[Rh(η^5-C_5H_5)(Bpin)(H)(PMe_2Ph)] 2. An NMR tube was charged with **1** (3 mg) and HBpin (ca. 1 mL) and irradiated at −10 °C for 3 h. The HBpin was removed under vacuum to give a dark-brown solid. NMR (C_6D_6, 300 K), ^{1}H: δ 7.7−6.98 (m, 5 H, C_6H_5), 5.35 (s, 5 H, C_5H_5), 1.75 (dd, 3H, J_{PH} = 10.4, J_{RhH} = 1.2 Hz, PMe_2Ph), 1.54 (d, 3H, J_{PH} = 9.7 Hz, PMe_2Ph), 1.11 (s, 12H, $BO_2C_6H_{12}$), −13.74 (dd, 1 H, J_{PH} = 32.1, J_{RhH} = 35.1 Hz, RhH). ^{31}P{^{1}H}: δ 26.3 (d, J_{RhP} = 173 Hz); ^{11}B{^{1}H}: δ 41.6.

[Rh(η^5-C_5H_5){PhP(2*R*,5*R*-$Me_2C_5H_6$)}(C_2H_4)] 3. {PhP(2*R*,5*R*-$Me_2C_5H_6$)} was synthesized by a literature procedure and used without distillation.[59] Complex **3** was synthesized by following literature procedures for the PMe_3 analogue, but replacing Tl(η^5-C_5H_5) by Li-(η^5-C_5H_5). The product was purified by passing through a silica column eluted with acetonitrile.[57,58] NMR (C_6D_6, 300 K), ^{1}H, 700 MHz: δ 7.7−7.09 (m, 5H, C_6H_5), 5.09 (s, 5H, C_5H_5), 2.83 (t, 1H, J_{HH} = 9.5 Hz, J_{PH} = 9.7 Hz, C_2H_4), 2.73 (t, 1H, J_{HH} = 9.5 Hz, J_{PH} = 10 Hz, C_2H_4), 2.29 (m, 1H, H^3), 1.82 (m, 1H, H^4), 1.54 (dd, J_{HH} = 7.5 Hz, J_{PH} = 10.5 Hz, 1H, C_2H_4), 1.46 (m, 2H, $H^{5'}$ and H^6), 1.34 (dd, J_{HH} = 7.2 Hz, J_{PH} = 18.2 Hz, 3H, H^7), 1.30 (dd, J_{HH} = 7.1 Hz, J_{PH} = 11.1 Hz, 1H, C_2H_4), 1.00 (m, 1H, $H^{4'}$), 0.89 (m, 1H, H^5), 0.57 (dd, J_{HH} = 6.6 Hz, J_{PH} = 13.3 Hz, 3H, H^8). ^{31}P{^{1}H}, 202.45 MHz: δ 75.2 (d, J_{RhP} = 203 Hz). ^{13}C, 176.04 MHz: δ 135.8 (d, J_{PC} = 27 Hz, *ipso*-Ph), 133.7 (d, J_{PC} = 11 Hz, *o*-Ph), 129.1 (s, *p*-Ph), 127.3 (d, J_{PC} = 9 Hz, *m*-Ph), 86.2 (s, C_5H_5), 35.1 (s, CH_2), 34.3 (s, CH_2), 32.3 (d, J_{PC} = 27 Hz, CH), 31.2 (d, J_{PC} = 24 Hz, CH), 24.6 (d, J_{PC} = 15 Hz, C_2H_4), 22.8 (d, J_{PC} = 15 Hz, C_2H_4), 22.1 (d, J_{PC} = 11 Hz, CH_3), 15.8 (s, CH_3). Mass spectrum, (EI, *m*/*z*): 388 (10%, M^+), 360 (100%, $M^+ - C_2H_4$).

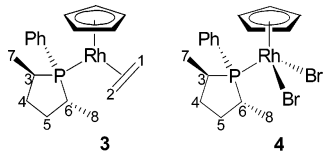

3 **4**

[Rh(η^5-C_5H_5)Br_2){PhP(2*R*,5*R*-$Me_2C_5H_6$)}] 4. An NMR tube was charged with **3** (5−6 mg) and 1,2-dibromoethane (∼1 mL) and irradiated at room temperature for 3 h. All volatiles were removed under vacuum giving an orange solid. Crystals were grown by slow evaporation of an ether solution. NMR (C_6D_6, 300 K): ^{1}H δ 7.8−7.0 (m, 5H, C_6H_5), 4.61 (s, 5H, C_5H_5), 3.68 (m, 1H, H^6), 2.43 (m, 1H, H^3), 2.31 (m, 1H, H^5), 1.67 (m, 2H, H^4 and $H^{5'}$), 1.20 (dd, J_{PH} = 17.6 Hz, J_{HH} = 6.5 Hz, 3H, H^7), 1.10 (dd, J_{PH} = 16.4 Hz, J_{HH} = 7 Hz, 3H, H^8), 0.88 (m, 1H, $H^{4'}$). ^{31}P{^{1}H}: δ 49.5 (d, J_{RhP} = 133 Hz). Mass Spectrum, quoted for ^{81}Br *m*/*z*: 522 (5%, M^+), 441 (30%, M^+-Br), 357 (45%), 284 (100%). HRMS *m*/*z*: experimental, 521.8829; calcd for $C_{17}H_{22}P^{81}Br_2Rh$, 521.8400; difference, 1.1 mDa. Anal. Calcd for $C_{17}H_{22}PBr_2Rh$: C, 39.26; H, 4.26. Found: C, 39.85; H, 4.82.

[Rh(η^5-C_5H_5)(Bpin)(H){PhP(2*R*,5*R*-$Me_2C_5H_6$)}] 5. An NMR tube was charged with **3** (5−6 mg) and HBpin (ca. 1.5 mL) and irradiated at room temperature. The reaction was followed by ^{31}P{^{1}H} NMR spectroscopy and was complete after 3 h irradiation. All volatiles were removed under vacuum giving a brown oil containing isomers **5a** and **5b** in proportions 2:1, respectively, and traces of boron-containing impurities. NMR (C_6D_6, 300 K) (superscript a and b indicate isomers **5a** and **5b**): ^{1}H δ 7.8−7.1 (m, 10 H, C_6H_5), 5.41, (s, 5H, $C_5H_5{}^b$) 5.40 (s, 5H, $C_5H_5{}^a$), 2.57 (m, 2H, $CH_2{}^{a,b}$ or $CH^{a,b}$), 2.01 (m, 2H, $CH_2{}^{a,b}$ or $CH^{a,b}$), 1.65 (m, 2H, $CH_2{}^{a,b}$ or $CH^{a,b}$), 1.52 (m, 2H, $CH_2{}^{a,b}$ or $CH^{a,b}$), 1.42 (dd, J_{PH} = 18.3 Hz, J_{HH} = 7.4 Hz, 3H, $CH_3{}^a$), 1.31 (m, 2H, $CH_2{}^{a,b}$ or $CH^{a,b}$), 1.21 (dd, J_{PH} = 18.9 Hz, J_{HH} = 7.35 Hz, 3H, $CH_3{}^b$), 1.10 (s, 6H, $BO_2C_6H_{12}{}^b$), 1.09 (s, 6 H, $BO_2C_6H_{12}{}^b$), 0.99 (s, 6H, $BO_2C_6H_{12}{}^a$), 0.98 (s, 6H, $BO_2C_6H_{12}{}^a$), 0.82 (dd, J_{PH} = 14.6 Hz, J_{HH} = 7.3 Hz, 3H, $CH_3{}^b$), 0.69 (dd, J_{PH} = 14.6 Hz, J_{HH} = 6.8 Hz, 3H, $CH_3{}^a$), −13.58 (dd, J_{PH} = 30 Hz, J_{RhH} = 34.4 Hz, 1H, RhH^a), −14.25 (dd, J_{PH} = 29 Hz, J_{RhH} = 34.4 Hz, 1H, RhH^b); two hydrogens obscured. ^{31}P{^{1}H}: δ 84.7 (d, J_{RhP} = 179 Hz, P^b), δ 82.6 (d, J_{RhP} = 174 Hz, P^a). ^{11}B δ 41.7^{a,b}.

[Rh(η^5-C_5H_5)$(H)_2${PhP(2*R*,5*R*-$Me_2C_5H_6$)}] 6. Complex **4** (20 mg, 0.039 mmol) was dissolved in toluene (15 mL) and $NaBH_4$ (9 mg, 0.24 mmol) added. Ethanol (50 mL) was added resulting in a color change from orange to light brown and release of hydrogen. The solution was stirred for 1 h at room temperature. The volatiles were removed in vacuo and hexane added (50 mL). The solid was removed by filtration and the hexane extracted was purified by elution through a short alumina column (ca. 4 cm length, neutral alumina) with hexane, toluene, and finally THF. The product was pumped to dryness and redissolved in C_6D_6 for NMR spectroscopy. NMR (C_6D_6, 300 K): ^{1}H, δ 7.8−7.1 (m, 5H, C_6H_5), 5.29 (s, 5H, C_5H_5), 2.29 (m, 1H, CH_2 or CH), 2.06 (m, 1H, CH_2 or CH), 1.80 (m, 1H, CH_2 or CH), 1.55 (m, 1H, CH_2 or CH), 1.25 (m, 1H, CH_2 or CH), 1.16 (dd, J_{HH} = 18.3, 6.9 Hz, 3H, CH_3), 1.04 (m, 1H, CH_2 or CH), 0.65 (dd, J_{HH} = 15.3, 7.1 Hz, 3H, CH_3), −13.71 (dd, J_{PH} 27.8, J_{RhH} 36.1 Hz, 1H, hydride), −14.47

(53) Green, M. L. H.; Wong, L. L.; Sella, A. *Organometallics* **1992**, *11*, 2660.
(54) Jeener, J.; Meier, B. H.; Bachmann, P.; Ernst, R. R. *J. Chem. Phys.* **1979**, *71*, 4546.
(55) Wagner, R.; Berger, S. *J. Magn. Reson.* **1996**, *A 123*, 119.
(56) Perrin, C. L.; Dwyer, T. J. *Chem. Rev.* **1990**, *90*, 935.
(57) Werner, H.; Feser, R. *J. Organomet. Chem.* **1982**, *232*, 351.
(58) Oliver, A. J.; Graham, W. A. G. *Inorg. Chem.* **1971**, *10*, 1165.
(59) Burk, M. J.; Feaster, J. E.; Harlow, R. L. *Tetrahedron Asymmetry* **1991**, *2*, 569.

(dd, J_{PH} 28.0, J_{RhH} 37.9 Hz, 1H, hydride). $^{31}P\{^1H\}$, 283.4 MHz, δ 84.0, d (J_{RhP} 159 Hz).

Computational Details. All calculations were performed with the Gaussian 03 package[60] of programs with the hybrid B3PW91 functional.[46] The calculations on the structures and energetics of (R_{Rh})-**5**, (S_{Rh})-**5**, **TS3**, **6**, and **TS4** were performed with the QM/MM(ONIOM) method,[61] with the phenyl group and all methyl substituents treated at the Universal Force Field (UFF) level.[62] The remaining parts were treated at the B3PW91 level. Single point DFT (B3PW91 or MPW2PLYP) calculations were carried out on QM/MM optimized structures. The rhodium atom was represented by the relativistic effective core potential (RECP) from the Stuttgart group (17 valence electrons) and its associated basis set,[63] augmented by an *f* polarization function ($\alpha = 1.350$).[64] The phosphorus atom was represented by RECP from the Stuttgart group and the associated basis set,[65] augmented by a *d* polarization function ($\alpha = 0.387$).[66] The remaining atoms (C, H, B, O) were represented by a 6-31G(*d*, *p*) basis set.[67] Full optimization of geometry was performed without any constraint, followed by analytical computation of the Hessian matrix to identify the nature of the located extrema as minima or transition states on the potential energy surface. To establish the nature of the connected intermediates, each transition state geometry was slightly perturbed along the TS vector in both directions and optimized as local minimum; perturbation was carried out by the IRC method or manually. Unless otherwise stated, only electronic energy values *E* are given. Values of *H* and *G* show the same trends. Natural bonding orbital analysis[68] was performed with the NBO 5.0 version implemented in Gaussian 03.

X-ray Cystallography. Diffraction data were collected on a Bruker Smart Apex diffractometer with Mo Kα radiation ($\lambda = 0.710\ 73$ Å) using a SMART CCD camera. Diffractometer control, data collection, and initial unit cell determination was performed using "SMART" (v5.625 Bruker-AXS). Frame integration and unit-cell refinement software was carried out with "SAINT+" (v6.22, Bruker AXS). Absorption corrections were applied using SADABS (v2.03, Sheldrick). The structure was solved by direct methods using SHELXS-97 (Sheldrick, 1997) and refined by full-matrix least-squares using SHELXL-97 (Sheldrick, 1997).[69] Hydrogen atoms were placed using a "riding model" and included in the refinement at calculated positions. Crystal data for **4**: $C_{17}H_{22}Br_2PRh$, fw = 520.05, $T = 110(2)$ K, orthorhombic, space group $P2(1)2(1)2(1)$, $a = 9.817(4)$ Å, $b = 12.992(5)$ Å, $c = 14.271(5)$ Å, $V = 1820.0(12)$ Å^3, $Z = 4$, $\rho_{calcd} = 1.898$ Mg m^{-3}, $\mu = 5.409$ mm^{-1}, $F(000) = 1016$, crystal size = 0.17 × 0.10 × 0.09 mm^3, $\theta = 2.12$ to 30.10°, independent reflections = 5289, parameters = 192, GOF = 1.011, final $R_1 = 0.0225$, $wR_2 = 0.0511$, absolute structure parameter = 0.047(5). CCDC no. 661280.

Acknowledgment. We appreciated assistance and discussions with Simon Duckett, Todd Marder, Christophe Raynaud, and Sylviane Sabo-Etienne. U.H. thanks the German Academic Exchange Service (DAAD) for a postdoctoral fellowship. We thank the CNRS, the French Ministry of National Education, and the European Commission for funding.

Supporting Information Available: Complete ref 60; figures for ^1H and ^{31}P NMR spectra of **3**, 2D NMR spectra of **3**, ^1H and ^{31}P NMR spectra of **5**, ^1H EXSY spectra of **6**, Eyring plot for **6**; tables of selected NMR data, equilibrium constants, and rate constants for interconversion of **5a**, **5b**, and **6**; Cartesian coordinates for the calculated structures; X-ray crystallographic files for **4** (CIF). This material is available free of charge via the Internet at http://pubs.acs.org.

JA077357O

(60) Pople, J. A.; et al. *Gaussian 03*, revision C.02, Gaussian Inc.: Wallingford, CT, 2004.
(61) Svensson, M.; Humbel, S.; Fröse, R. D. J.; Matsubara, T.; Sieber, S.; Morokuma, K. *J. Phys. Chem.* **1996**, *100*, 19357.
(62) Rappé, A. K.; Casewit, C. J.; Colwell, K. S.; Goddard, W. A., III; Skiff, W. M. *J. Am. Chem. Soc.* **1992**, *114*, 10024.
(63) Andrae, D.; Häussermann, U.; Dolg, M.; Stoll, H.; Preuss, H. *Theor. Chim. Acta* **1990**, *77*, 123.
(64) Ehlers, A. W.; Böhme, M.; Dapprich, S.; Gobbi, A.; Höllwarth, A.; Jonas, V.; Köhler, K. F.; Stegmann, R.; Veldkamp, A.; Frenking, G. *Chem. Phys. Lett.* **1993**, *208*, 111.
(65) Bergner, A.; Dolg, M.; Kuchle, W.; Stoll, H.; Preuss, H. *Mol. Phys.* **1993**, *80*, 1431.
(66) Höllwarth, A.; Böhme, H.; Dapprich, S.; Ehlers, A. W.; Gobbi, A.; Jonas, V.; Köhler, K. F.; Stegmann, R.; Veldkamp, A.; Frenking, G. *Chem. Phys. Lett.* **1993**, *208*, 237.
(67) Hariharan, P. C.; Pople, J. A. *Theor. Chim. Acta* **1973**, *28*, 213.
(68) Reed, A. E.; Curtis, L. A.; Weinhold, F. *Chem. Rev.* **1988**, *88*, 899.
(69) Sheldrick, G. M. *SHELXS-97, Program for Structure Solution*; University of Göttingen: Göttingen, Germany, 1997. Sheldrick, G. M. *SHELXL-97: Program for the Refinement of Crystal Structures*; University of Göttingen: Göttingen, Germany, 1997.